



University of Groningen

Tinnitus-related dissociation between cortical and subcortical neural activity in humans with mild to moderate sensorineural hearing loss

Boyen, Kris; de Kleine, Emile; van Dijk, Pim; Langers, Dave R. M.

Published in:
Hearing Research

DOI:
[10.1016/j.heares.2014.03.001](https://doi.org/10.1016/j.heares.2014.03.001)

IMPORTANT NOTE: You are advised to consult the publisher's version (publisher's PDF) if you wish to cite from it. Please check the document version below.

Document Version
Publisher's PDF, also known as Version of record

Publication date:
2014

[Link to publication in University of Groningen/UMCG research database](#)

Citation for published version (APA):

Boyen, K., de Kleine, E., van Dijk, P., & Langers, D. R. M. (2014). Tinnitus-related dissociation between cortical and subcortical neural activity in humans with mild to moderate sensorineural hearing loss. *Hearing Research*, 312, 48-59. <https://doi.org/10.1016/j.heares.2014.03.001>

Copyright

Other than for strictly personal use, it is not permitted to download or to forward/distribute the text or part of it without the consent of the author(s) and/or copyright holder(s), unless the work is under an open content license (like Creative Commons).

Take-down policy

If you believe that this document breaches copyright please contact us providing details, and we will remove access to the work immediately and investigate your claim.

Downloaded from the University of Groningen/UMCG research database (Pure): <http://www.rug.nl/research/portal>. For technical reasons the number of authors shown on this cover page is limited to 10 maximum.



Research paper

Tinnitus-related dissociation between cortical and subcortical neural activity in humans with mild to moderate sensorineural hearing loss

Kris Boyen^{a,b,*}, Emile de Kleine^{a,b}, Pim van Dijk^{a,b}, Dave R.M. Langers^{a,b,c}^a Department of Otorhinolaryngology/Head and Neck Surgery, University of Groningen, University Medical Center Groningen, The Netherlands^b Graduate School of Medical Sciences, Research School of Behavioural and Cognitive Neurosciences, University of Groningen, The Netherlands^c National Institute for Health Research (NIHR), Nottingham Hearing Biomedical Research Unit, University of Nottingham, Nottingham, UK

ARTICLE INFO

Article history:

Received 17 October 2013

Received in revised form

21 February 2014

Accepted 4 March 2014

Available online 12 March 2014

ABSTRACT

Tinnitus is a phantom sound percept that is strongly associated with peripheral hearing loss. However, only a fraction of hearing-impaired subjects develops tinnitus. This may be based on differences in the function of the brain between those subjects that develop tinnitus and those that do not. In this study, cortical and sub-cortical sound-evoked brain responses in 34 hearing-impaired chronic tinnitus patients and 19 hearing level-matched controls were studied using 3-T functional magnetic resonance imaging (fMRI). Auditory stimuli were presented to either the left or the right ear at levels of 30–90 dB SPL. We extracted neural activation as a function of sound intensity in eight auditory regions (left and right auditory cortices, medial geniculate bodies, inferior colliculi and cochlear nuclei), the cerebellum and a cinguloparietal task-positive region. The activation correlated positively with the stimulus intensity, and negatively with the hearing threshold. We found no differences between both groups in terms of the magnitude and lateralization of the sound-evoked responses, except for the left medial geniculate body and right cochlear nucleus where activation levels were elevated in the tinnitus subjects. We observed significantly reduced functional connectivity between the inferior colliculi and the auditory cortices in tinnitus patients compared to controls. Our results indicate a failure of thalamic gating in the development of tinnitus.

© 2014 The Authors. Published by Elsevier B.V. This is an open access article under the CC BY-NC-ND license (<http://creativecommons.org/licenses/by-nc-nd/3.0/>).

1. Introduction

Tinnitus is a poorly understood hearing disorder characterized by the presence of an auditory percept in the absence of an external stimulus and is typically associated with hearing loss. It is a common disorder with prevalence estimates ranging from 7 to 20% (Hoffman and Reed, 2004). Approximately 40% of the tinnitus patients also suffer from hyperacusis, a diminished tolerance to

ordinary environmental sounds (Baguley, 2003). Most patients with chronic tinnitus are continuously aware of the tinnitus percept, but are able to cope effectively with the disturbance. However, for some patients the tinnitus is more than a trivial annoyance resulting in feelings of desperation and even suicidal thoughts (Dobie, 2003).

An important role in the generation of tinnitus is currently attributed to mechanisms in the central auditory system. Animal studies have shown that manipulations that are known to be sources of tinnitus in humans (e.g. noise trauma) cause increased spontaneous neural activity or changes in neural synchrony in auditory brain structures (Noreña and Eggermont, 2003; Seki and Eggermont, 2003). A number of blood oxygenation level dependent (BOLD) functional magnetic resonance imaging (fMRI) studies have investigated the neural correlates of tinnitus in humans (for a review, see Lanting et al., 2009; Adjamian et al., 2009). BOLD fMRI is unable to register sustained increases in spontaneous activity. Consequently, these fMRI studies applied sound stimuli to probe abnormal sound processing in the brain of tinnitus patients. Measuring changes in hemodynamics as a response to sound in tinnitus sufferers revealed increased activation in the inferior

Abbreviations: AC, auditory cortex; ANCOVA, analysis of covariance; BA, Brodmann area; BOLD, blood oxygenation level dependent; CER, cerebellum; CN, cochlear nucleus; DMN, default mode network; fMRI, functional magnetic resonance imaging; EPI, echo planar imaging; FWE, family wise error; HI, hearing-impaired; HI + T, hearing-impaired and tinnitus; IC, inferior colliculus; L, left; MGB, medial geniculate body; MNI, Montreal neurological institute; PTA, pure-tone average; R, right; ROI, region of interest; TPN, task-positive network; THI, tinnitus handicap inventory

* Corresponding author. Department of Otorhinolaryngology/Head and Neck Surgery, University of Groningen, University Medical Center Groningen, P.O. Box 30.001, 9700 RB Groningen, The Netherlands. Tel.: +31 50 3613290; fax: +31 503611698.

E-mail address: k.boyen@umcg.nl (K. Boyen).

<http://dx.doi.org/10.1016/j.heares.2014.03.001>

0378-5955/© 2014 The Authors. Published by Elsevier B.V. This is an open access article under the CC BY-NC-ND license (<http://creativecommons.org/licenses/by-nc-nd/3.0/>).

colliculus compared to controls (Melcher et al., 2000, 2009; Lanting et al., 2008), although this may have been associated with hyperacusis rather than with tinnitus (Gu et al., 2010). In contrast to activation of the brainstem, elevated sound-evoked auditory cortex activation can be attributed to tinnitus (Gu et al., 2010). These studies all show neural correlates of tinnitus in clinically normal-hearing subjects.

The majority of tinnitus patients, however, has a significant hearing loss. As was shown in numerous animal studies, hearing loss is associated with adaptation in the central auditory system, which is likely to be related to tinnitus (for a review, see Eggermont, 2001). Since tinnitus does not develop in all hearing-impaired individuals, it must be assumed that these adaptations are different between those that develop tinnitus and those that do not. So far, differences in adaptations are supported by two models on the pathophysiology of tinnitus: one based on abnormal thalamic gating (Rauschecker et al., 2010; Zhang, 2013) and another based on thalamic hypo-activity (Llinás et al., 1999).

The aim of this explorative study was to investigate tinnitus-related abnormalities in sound-evoked hemodynamic responses in subjects with mild to moderate sensorineural hearing loss. Two relatively large subject groups were enrolled: a hearing-impaired group without tinnitus and a hearing-impaired group suffering from tinnitus. Both groups were carefully matched with respect to age and hearing loss, which allows us to identify the effects that are specific to tinnitus. In line with previous studies (Melcher et al., 2000, 2009; Lanting et al., 2008; Gu et al., 2010), we used BOLD fMRI to measure sound-evoked responses throughout the brain, and primarily focused on auditory regions since we used auditory stimuli. Differences between both groups were investigated with respect to the magnitude of brain responses, their lateralization, and the functional connectivity patterns between brain regions.

2. Materials and methods

2.1. Subjects

This study included data collected from two groups of patients. The patients were recruited at the University Medical Center Groningen and via hearing aid dispensers in Groningen, the Netherlands. The first group comprised 19 hearing-impaired subjects (HI group). The second group comprised 34 subjects with a hearing impairment suffering from tinnitus (HI + T group). From the same subjects, the T1 anatomical scans of 16 HI and 31 HI + T subjects have also been included in a previous morphological study (Boyen et al., 2013). Pure-tone audiometry was performed with a clinical audiometer using six different octave frequencies (0.25, 0.5, 1, 2, 4 and 8 kHz). For all subjects, the pure-tone average (PTA) hearing threshold at the octave frequencies of 1, 2 and 4 kHz satisfied $30 \leq \text{PTA} \leq 60$ dB in both ears.

To assess handedness, a translated version of the Edinburgh Inventory (Oldfield, 1971) was completed by all subjects. In the tinnitus subjects only, tinnitus handicap was assessed by a Dutch translation of the Tinnitus Handicap Inventory (THI), a self-reported tinnitus handicap questionnaire (Newman et al., 1996). In order to assess the presence of hyperacusis, a translated version of the Hyperacusis Questionnaire (HQ; Khalfa et al., 2002) was administered to all participating subjects. Furthermore, the subjectively perceived tinnitus loudness was recorded on a numeric rating scale from zero (tinnitus not audible at the time) to ten (tinnitus sounds as loud as imaginable) before and immediately after the scanning session. None of the subjects had any major medical, neurological or psychiatric history.

This study was approved by the local medical ethics committee. All subjects were informed about the purpose of the study before giving their written consent in accordance with Dutch legislation.

2.2. Data acquisition

The imaging experiments were performed using a 3-T MRI system (Philips Intera, Philips Medical Systems, Best, The Netherlands) which was equipped with an eight-channel phased-array (SENSE) head coil. The functional scans consisted of 2200-ms single-shot T_2^* -sensitive echo planar imaging (EPI) sequences with 41 3-mm thick slices (TR 10 s; TE 22 ms; flip-angle 80° ; voxel size $1.75 \times 1.95 \times 3$ mm³; field of view $224 \times 224 \times 123$ mm³) and were acquired using a near-coronal orientation, aligned to the brainstem when viewed on a midsagittal cross-section. Each image volume enclosed left and right cochlear nuclei (CN), inferior colliculi (IC), medial geniculate bodies (MGB) and auditory cortices (AC). The influence of acoustic scanner noise was reduced using a sparse sampling strategy (Hall et al., 1999; Langers et al., 2005a). Auditory stimuli were presented during a 7.8-s gap of scanner silence between two successive acquisitions. For each subject, three runs of 73 acquisitions were performed. Additional start-up scans that were included to achieve magnetization equilibrium and to trigger the start of the stimulus delivery were excluded from analysis. In addition, a 3-dimensional high-resolution T_1 -weighted fast-field echo scan (TR 9 ms; TE 3.50 ms; flip-angle 8° ; voxel size $1 \times 1 \times 1$ mm³; field of view $256 \times 256 \times 170$ mm³) was acquired with the same orientation as the functional scans to serve as an anatomical reference.

2.3. Acoustic stimulation and scanning paradigm

Auditory stimuli were delivered by an MR-compatible electrodynamic system (MR Confon GmbH, Magdeburg, Germany; Baumgart et al., 1998), connected to a PC setup equipped with a digital-to-analog converter controlled by Labview 6.1 (National Instruments 6052E, National Instruments Corporation, Austin, TX, USA). The stimuli consisted of dynamic ripples (Langers et al., 2003). The spectrum of a dynamic ripple is based on pink noise, but contains temporal and spectral modulations. The stimuli comprised frequency components between 125 and 8000 Hz, with a spectral modulation density of one cycle per octave, a temporal modulation frequency of two cycles per second, and a modulation amplitude of 80%. These stimuli were chosen for their potency to induce robust sound-evoked responses in the auditory pathway (Langers et al., 2003; Lanting et al., 2008, 2010).

During the gaps of scanner silence between two successive acquisitions, auditory stimuli were presented to the left (L) or the right (R) ear at either 30, 50, 70 or 90 dB SPL (L_{30} , L_{50} , L_{70} , L_{90} ; R_{30} , R_{50} , R_{70} or R_{90}). In addition, a silent baseline condition was included. The stimuli were presented in a fixed pseudo-random order in each functional run. Per run, the silent condition was presented nine times and all the stimulus conditions were presented eight times each. During the functional scans, the subjects were instructed to register whether they perceived an audible stimulus using a button box: whenever they perceived an audible stimulus in the left or right ear, they pressed one of two corresponding buttons with their right thumb. This task was imposed in order to promote and monitor that the subject paid attention to the presented sound stimuli.

2.4. Data processing and linear regression analysis

The images were analyzed using SPM8 (Functional Imaging Laboratory, The Wellcome Department of Imaging Neuroscience,

London, UK, <http://www.fil.ion.ucl.ac.uk/spm/>) and MatLab 7.1 (The Mathworks Inc., Natick, MA). The functional images were first corrected for motion using realignment on the basis of 3-D rigid body transformations. The T_1 -weighted high-resolution anatomical images were spatially co-registered to the functional images, and all images were normalized into Montreal Neurological Institute (MNI) stereotaxic space. To improve the signal-to-noise ratio, the functional data were spatially smoothed using an isotropic Gaussian kernel with a full width at half maximum of 4 mm. In order to express the signal measures in percentage signal change, a logarithmic transformation was carried out (Langers and van Dijk, 2011). The functional images were interpolated to voxel dimensions of $2.0 \times 2.0 \times 2.0 \text{ mm}^3$.

Per subject, a general linear model was set up to analyze the relative contribution of each condition to the measured response. The model included one covariate for each of the eight stimulus conditions, the realignment parameters, as well as constant and linear terms to model the baseline and drift within each run. An omnibus F -test, including contrasts of all individual stimulus conditions relative to baseline, was assessed in each voxel to detect the combined effect of all sound stimuli. The confounds (i.e. baseline, drift and realignment) that were estimated were subtracted from the preprocessed functional acquisitions for the purpose of subsequent connectivity analyses.

The contrast images of the eight sound conditions of interest, relative to the silent condition, were entered in a second-level random-effects analysis based on a flexible factorial design with factors for group (i.e. HI + T and HI), subject, and stimulus condition. Significant responses to all sound conditions across all subjects were detected by means of an F -test.

2.5. ROI definitions and functional connectivity

Eight regions of interest (ROIs) were defined, comprising both left and right auditory cortex (AC), medial geniculate body (MGB), inferior colliculus (IC) and cochlear nucleus (CN). The ROIs of the left and right AC, MGB and IC were defined by means of the outcomes of the second-level random-effects analysis (see Results). The AC ROI comprised all supra-threshold voxels in the temporal lobe ($F_{7,357} > 6.53$; $p < 0.05$ corrected for family-wise errors). The MGB and IC ROIs were drawn to include a cluster of supra-threshold voxels around the correspondingly localized activation maxima. Because no activation of the left or right CN was found, these ROIs were defined as a sphere with a radius of 5 mm positioned at MNI coordinates ($\pm 10, -38, -45$) consistent with a previous publication of our group (Boyen et al., 2013).

Next, functional connectivity analysis was performed. Functional connectivity examines the correlations among activity in different brain areas (Friston, 1994; Smith et al., 2009). Time courses were determined for all auditory ROIs by averaging the preprocessed hemodynamic signals of all voxels in the respective ROI and concatenating them across all subjects. For each ROI, a functional connectivity map was derived by calculating the Pearson correlation coefficients R between the time course of the respective ROI and the time courses of all other voxels in the brain.

Based on the group connectivity maps (see Section 3.3), two more ROIs were included: the cerebellum (CER) and a task-positive network (TPN) region, a term adopted from, inter alia, Fox et al. (2005). The ROI of the CER consisted of the anterior and posterior cerebellar lobes. The TPN comprised the bilateral cingulate cortex, the primary somatosensory cortex (Brodmann Areas (BAs) 1, 2 and 3), the primary motor cortex (BA 4) and the supplementary motor area (BA 6). Both ROIs (CER and TPN) were defined according to the WFU_pickatlas (Maldjian et al., 2003).

Table 1

Subjects' characteristics. Hearing loss was measured as the pure-tone average (PTA) hearing threshold at the octave frequencies 1, 2 and 4 kHz. The mean values with standard deviation are listed. HI + T: hearing impairment accompanied by tinnitus; HI: hearing-impaired; THI: Tinnitus Handicap Inventory; HQ: Hyperacusis Questionnaire.

	HI + T (n = 34)	HI (n = 19)
Age		
Years	57 ± 10	62 ± 12
Range	31–75	44–84
Gender		
Male	21	16
Female	13	3
Handedness		
Right	28	16
Left	2	1
Ambidextrous	4	2
Hearing loss (dB HL)		
Right ear	41 ± 8	44 ± 11
Left ear	42 ± 10	45 ± 8
HQ score (0–42)		
Score	20 ± 7	15 ± 8
Range	5–33	2–30
THI score (0–100)		
Score	31 ± 22	–
Range	4–72	–

2.6. Response amplitudes and lateralization of regions-of-interest

For each subject, the 10% most strongly responding voxels within each ROI according to the individual F -test were selected (see Table 3), and per condition the signal change relative to baseline was averaged over these voxels. Following previous studies (Langers et al., 2005b; Lanting et al., 2008; Norman-Haignere et al., 2013), we chose to use a fixed percentage of voxels instead of a fixed significance threshold because differences in significance values across subjects are partly driven by nonspecific differences in signal-to-noise ratio that are unrelated to neural activity. Statistical analyses were performed using a repeated measures ANCOVA model for each ROI separately. In addition to the factors for group, subject and stimulus condition that were included in the second-level random-effects model already, this model included the subject's PTA hearing loss in the ear of stimulus presentation as a covariate. The main effects of group and stimulus condition and the interaction between these two factors were determined. In addition, we tested whether neural activation in response to the stimuli co-varied with the amount of hearing loss in the ear of presentation.

For each ROI of each subject, the average response to all stimuli presented to the left (L) and the right (R) ear, respectively, was calculated. The values obtained were used to calculate a lateralization index

Table 2

Number of times that the button was pressed, expressed in percentages. The percentages are shown for each group and each stimulus condition, respectively. HI + T: hearing-impaired chronic tinnitus patients; HI: hearing level-matched controls without tinnitus.

	HI + T		HI	
	Left ear [%]	Right ear [%]	Left ear [%]	Right ear [%]
30 dB SPL	14	19	16	8
50 dB SPL	52	53	58	52
70 dB SPL	95	94	100	95
90 dB SPL	100	100	100	100

Table 3

Results of the regression analysis and repeated measures ANCOVA for each ROI. The number of the 10% most strongly responding voxels (N), the regression coefficients (β) of the activation as a function of the left and right ear stimulus level and the hearing loss in the stimulated ear and the significance (p) of each factor (G : group; S : stimulus; $G \times S$: group–stimulus interaction) or covariate (HL: the subject's PTA hearing loss in the ear of stimulus presentation) according to an ANCOVA are listed. Significant results ($p < 0.05$) are underlined. AC: auditory cortex; MGB: medial geniculate body; IC: inferior colliculus; CN: cochlear nucleus; TPN: task-positive network; CER: cerebellum.

	$N [2 \times 2 \times 2 \text{ mm}^3]$	Regression coefficient, $\beta [10^{-3}\%/\text{dB SPL}]$			Significance, $p [-]$			
		Left ear	Right ear	Hearing loss	G	S	$G \times S$	HL
Left AC	499	<u>20</u>	<u>32</u>	−6.3	0.74	<0.001	0.50	0.14
Right AC	453	<u>32</u>	<u>19</u>	−2.1	0.62	<0.001	0.67	0.63
Left MGB	31	<u>5.1</u>	<u>5.9</u>	−7.2	<u>0.021</u>	<0.001	0.36	<0.001
Right MGB	27	<u>7.0</u>	<u>3.5</u>	−6.2	0.08	<0.001	0.45	<u>0.002</u>
Left IC	12	<u>3.4</u>	<u>6.5</u>	−5.4	0.23	<0.001	0.42	<u>0.001</u>
Right IC	15	<u>5.6</u>	<u>3.3</u>	−0.84	0.39	<0.001	0.45	0.62
Left CN	8	<u>4.4</u>	<u>4.4</u>	−7.5	0.15	<u>0.046</u>	0.50	<u>0.004</u>
Right CN	8	<u>3.8</u>	<u>3.7</u>	−13.9	<0.001	0.15	0.59	<0.001
TPN	17,402	<u>5.8</u>	<u>5.4</u>	−2.7	0.74	<0.001	0.46	0.15
CER	2241	<u>6.4</u>	<u>6.3</u>	−4.9	0.14	<0.001	0.52	<u>0.003</u>

$$LI = \frac{L - R}{|L| + |R|}$$

For positive responses, a value of +1 indicates a response to stimuli presented at the left ear only, whereas a value of −1 indicates a response to right-ear stimuli only. Group differences for the individual ROIs were tested for by means of two-tailed two-sample t -tests.

2.7. Network analysis

Pairwise Pearson correlations were calculated as a measure of functional connectivity between the various ROIs. For this analysis, the previously defined unilateral auditory ROIs were combined to bilateral ROIs because homologous areas in both hemispheres are known to be highly correlated. Within each of the six ROIs (four auditory ROIs, CER and TPN), the signals of the 10% most active voxels were averaged for each point in time (i.e. scan). The obtained fMRI time courses were transformed to zero mean and unit variance for each subject. Per group, these arrays were concatenated across the subjects belonging to the HI + T group and HI group respectively, resulting in a matrix $\mathbf{X}_{\text{HI}+\text{T}}$ of 10 time courses of 7446 elements in time (34 subjects \times 219 time points) and a matrix \mathbf{X}_{HI} of 10 time courses with each 4161 elements in time (19 subjects \times 219 time points).

Bootstrapping (Wu, 1986; Liu, 1988) was performed to test whether the correlation coefficients between the six ROIs were significantly different from zero within each group separately. In order to obtain a null-distribution for the correlation coefficients, the time courses of random subsets of runs (consisting of 73 points in time) were repeatedly negated for each ROI independently. For each iteration, a Pearson correlation between pairs of ROIs was calculated. A total of 50 000 iterations was performed to produce a null distribution. The obtained null-distribution was used to assess whether significance was reached ($p < 0.05$). A Bonferroni correction was applied for the total number of 15 connections in the model.

Non-parametric permutation tests (Good, 2002; Nichols and Holmes, 2002) were performed to test whether the correlation coefficients were significantly different between the subjects groups. A null distribution was obtained by randomly reassigning subjects to the two groups, while retaining the original group sizes. A total of 50 000 permutations was performed. For each iteration, the difference between the correlation coefficients was calculated. The obtained null-distribution was used to assess the significance of group difference ($p < 0.05$). A Bonferroni correction was applied for the total number of 15 connections in the model.

3. Results

3.1. Subject characteristics

The subjects included in this study had mild to moderate sensorineural hearing loss (see Fig. 1). Statistical analyses of group differences were performed by means of a two-tailed two-sample t -test (hearing thresholds and age) or a Fisher's exact test (gender and handedness). Statistical analysis of the hearing threshold at each of the octave frequencies (0.25, 0.5, 1, 2, 4 and 8 kHz, respectively) did not show significant differences between the subjects with and those without tinnitus ($p > 0.05$). An exact distribution-free test comparing two multivariate distributions (Rosenbaum, 2005) did not show significant differences in audiometric shape between both groups ($p = 0.73$), indicating that both groups were well matched in their mean audiometric thresholds as well as in their deviations from the mean. The two groups did not differ in age ($p = 0.07$), gender ($p = 0.12$), and handedness ($p = 1.00$). The HQ was filled out by all but two subjects belonging to the HI + T group. A significant difference between both groups was found ($p = 0.024$), with the HI + T group having higher scores relative to the HI group. Moreover, a correlation between the THI and HQ scores was found ($R = 0.61$; $p < 0.001$). Details of the participants' characteristics are listed in Table 1.

In both groups, the number of participating women is lower than the number of participating men, which is representative of the prevalence of tinnitus and hearing loss in the general population (Lockwood et al., 2002). Age was significantly correlated with hearing loss (regression coefficient $m = 0.30 \text{ dB/yr}$; $p = 1.9 \times 10^{-4}$). Out of the 34 tinnitus subjects, 25 subjects perceived tinnitus in both ears, seven subjects perceived tinnitus only in the left ear and two subjects perceived tinnitus only in the right ear. The tinnitus subjects suffered from chronic continuous tinnitus for at least one year up to 29 years. The subjectively perceived tinnitus loudness, as measured with a rating scale from zero to ten, was slightly but not significantly ($p = 0.52$) increased after scanning the subjects (5.5 ± 1.9 ; mean \pm SD) as compared to before the scan session (5.2 ± 2.0) (see Fig. 2).

During the functional scans, the subjects were instructed to press a button whenever they perceived an audible stimulus in the left or right ear. For each stimulus condition, Table 2 lists the percentage of times that the button was pressed by the subjects of a group.

3.2. Sound-evoked responses

The significant responses to the auditory stimuli are visualized in Fig. 3. Based on the F -test clear significant responses were

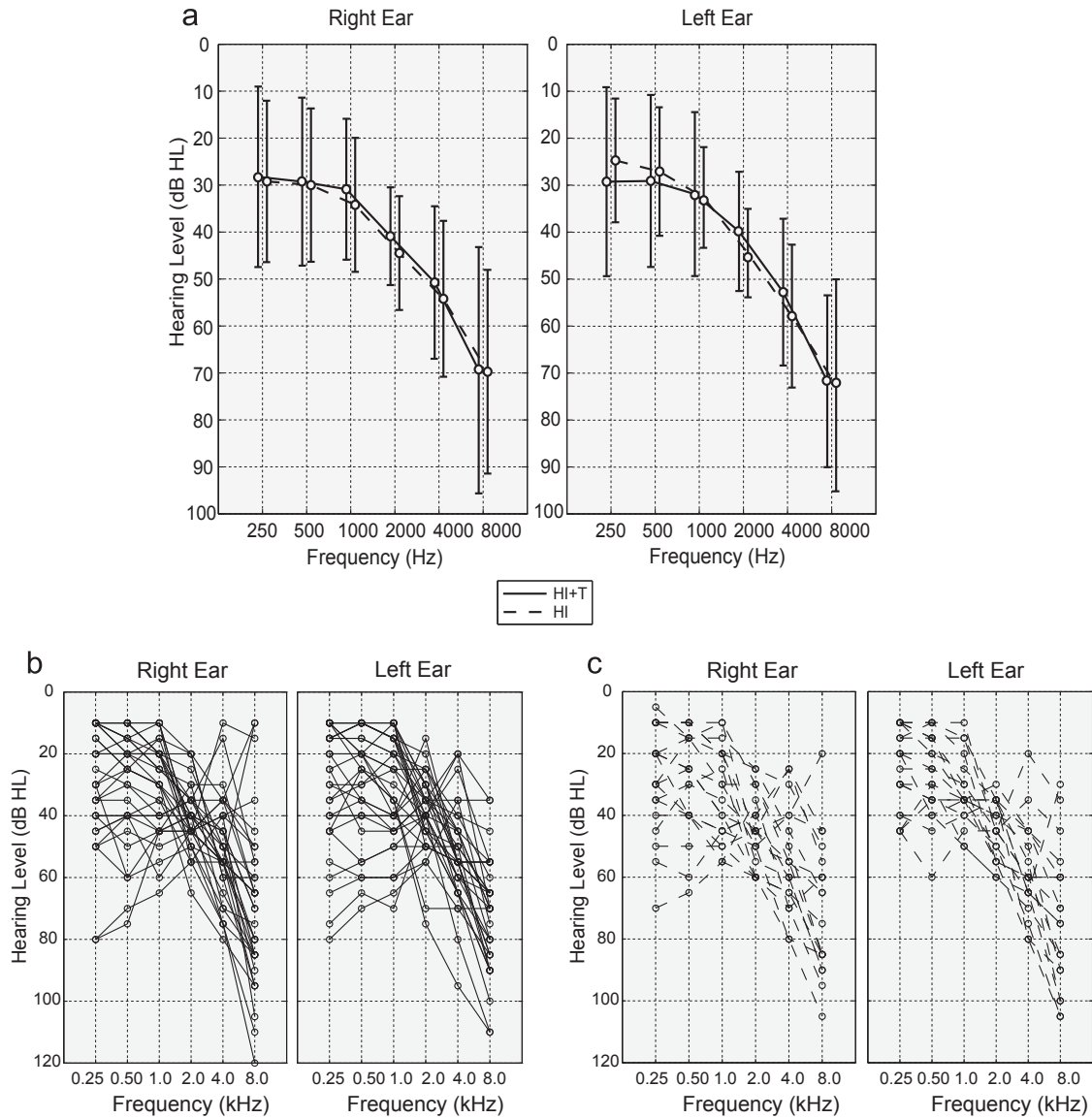


Fig. 1. Audiograms. a. Mean audiograms for the HI + T group (solid line) and HI group (dashed line). The error bars indicate the group standard deviations around the mean. b. Individual audiograms for the HI + T group. c. Individual audiograms for the HI group. HI + T: hearing impairment accompanied by tinnitus; HI: hearing-impaired subjects without tinnitus.

detected in the AC, MGB and IC. Responses in the CN did not reach significance. Additionally, significant responses in the parietal lobe and cerebellum were detected.

3.3. Functional connectivity maps

Pearson correlation coefficients were computed between the time course of each auditory seed ROI and the time courses of all voxels in the brain. The resulting maps, thresholded at an arbitrary level of $R = 0.25$, are presented in Fig. 4. The left and right AC are strongly correlated to voxels in the thalamus (MGB) and the midbrain (IC), but not with the lower brainstem (CN). The thalamus is connected to voxels in both the cortex and the midbrain and lower brainstem. Correspondingly, the regions in the midbrain and lower brainstem are connected to voxels in the thalamus, but not the cortex.

The auditory cortex and, to a lesser extent, the thalamus show extensive time course correlations with voxels in the cerebellum,

pericentral gyri and cingulate cortex. Moreover, the CN shows some time course correlations with voxels in the cerebellum. These regions were additionally included as two large separate ROIs (i.e. CER and TPN) in the ROI analysis and network analysis that followed.

3.4. Region-of-interest analysis

We performed ROI analyses on the eight ROIs in the auditory pathway and the two additional ROIs as defined following the seed-ROI connectivity maps. For each ROI, the mean percentage signal change for the various stimulus levels compared to baseline in both groups are shown in Fig. 5. In general, louder stimuli yielded larger responses in all ROIs. The TPN and CER showed a plateau effect: responses increased until the stimulus level equaled 70 dB, and subsequently remained at a similar level for the 90-dB stimulus.

For all ROIs, the regression coefficients of the activation as a function of the left and right ear stimulus level were positive

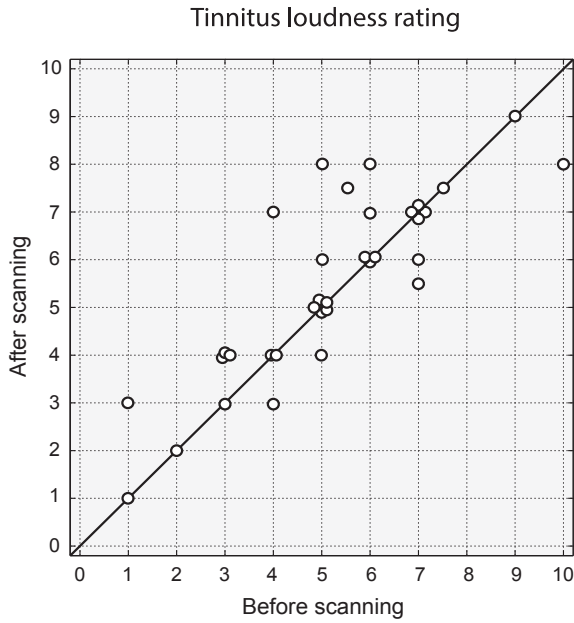


Fig. 2. Tinnitus loudness ratings before and after scanning. The ratings were measured by means of a numeric rating scale from zero (tinnitus not audible at the time) to ten (tinnitus sounds as loud as imaginable).

(Table 3). These positive slopes (β values) were significant for all ROIs except the right CN. For hearing loss, a negative regression coefficient was found in all auditory ROIs. Significance was reached in the CER and all auditory subcortical ROIs, except the right IC.

The repeated measures ANCOVA of the ROI responses (Table 3) showed no effect of subject group (HI vs. HI-T) except in the right CN and left MGB. A significant effect of stimulus condition was found in all ROIs except the right CN. In all subcortical auditory ROIs except the right IC, hearing loss had a significant effect on the responses. There was no effect of hearing loss in the auditory cortex.

In the non-auditory areas (TPN and CER), stimulus condition had a significant effect on the response, but hearing loss only affected the response in the CER. We also tried two alternative models in which THI, respectively HQ, was included as a covariate instead of hearing loss, but found no significant effects related to tinnitus, respectively hyperacusis, severity.

Fig. 6 shows the lateralization index for each ROI. The lateralization indices for both groups show a clear contralateral stimulus preference for the bilateral AC, MGB and IC. The right CN was ipsilaterally lateralized in both groups, whereas the left CN was not. The differences between the subject groups did not reach significance. For all nuclei, except the left MGB and bilateral CN, the HI group showed a stronger lateralization toward the left ear, compared to the HI + T group. The CER and TPN tended to lateralize to the left ear.

3.5. Network analysis

An overview of the functional connections for both groups is given in Fig. 7. All possible pairs of ROIs resulted in a significant positive correlation (Bonferroni-corrected $p < 0.05$). Successive connections within the auditory pathway tended to be stronger than non-successive connections. The nuclei of the brainstem (CN and IC) were relatively strongly correlated with each other and with the thalamus (MGB). The cortex (AC and TRN) and the thalamus were strongly correlated as well. However, the correlations between the cortex and the brainstem were relatively weak. In other words, the correlation analysis showed two clusters of auditory centers, with the thalamus belonging to both clusters. In both groups, the CER as well as the TPN showed the strongest connectivity with the auditory pathway at the level of the cortex. Thus, the CER and the TPN seem to belong to the corticothalamic cluster. Furthermore, the CER and the TPN were mutually highly correlated in both groups (HI + T: $R = 0.72$; HI: $R = 0.74$).

The significant difference between the HI + T and HI groups concerning the functional correlations is indicated by the white squares in Fig. 7. The correlation between the AC and the IC was

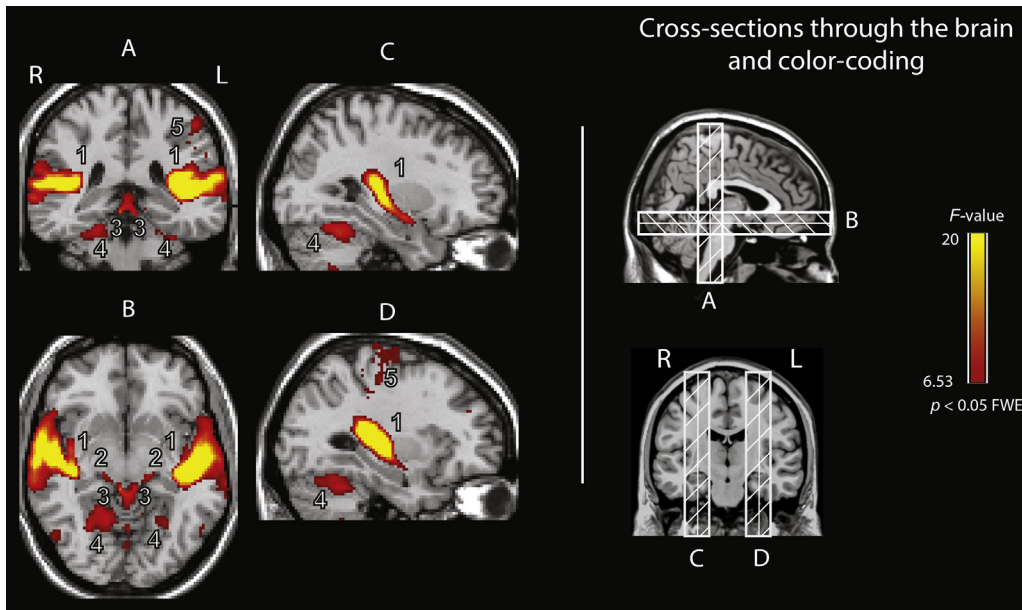


Fig. 3. Coronal, axial and sagittal cross-sections of the brain showing significant responses to sound across all stimulus conditions and all subjects by means of an F-test. In each image, the activation in 11 contiguous slices was projected on an anatomical background. The red–yellow color-coded areas indicate areas with a significant response; auditory cortex (1), medial geniculate body (2), inferior colliculus (3), cerebellum (4) and parietal region (5). The threshold was set at $p < 0.05$, corrected for family-wise errors (FWE). (For interpretation of the references to color in this figure legend, the reader is referred to the web version of this article.)

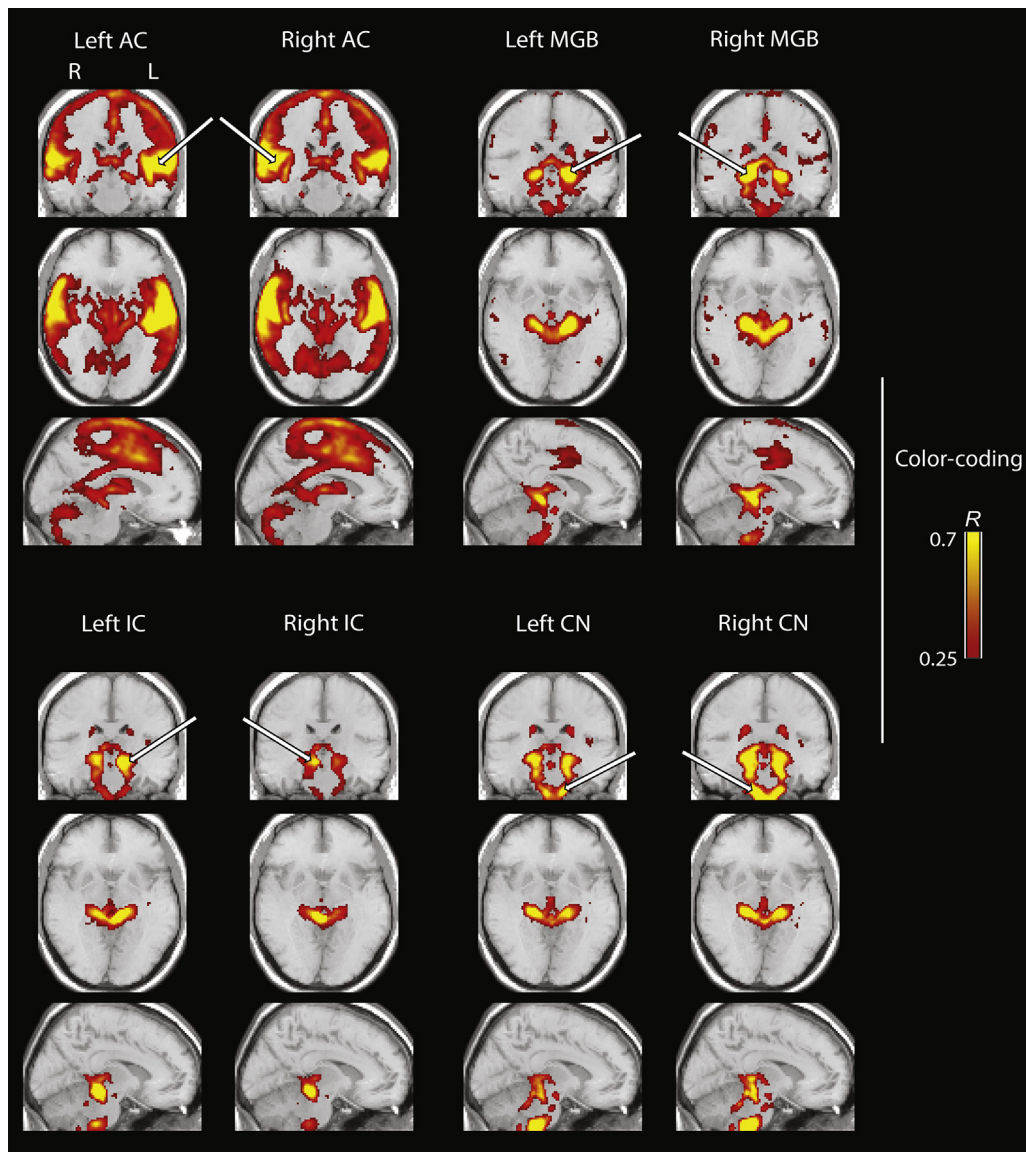


Fig. 4. Functional connectivity maps across all subjects. Eight auditory regions of interest (ROIs) were defined (indicated with the white arrows). Pearson correlation coefficients R were calculated between the time courses of the ROIs and those of every voxel in the brain. The correlation coefficients were thresholded at a level of 0.25, and overlaid on coronal, axial and transversal cross-sections. The red–yellow color-coded areas indicate functionally connected voxels with the respective ROI. Each ROI highly correlated with its constituent voxels and is thus yellow-colored. AC: auditory cortex; MGB: medial geniculate body; IC: inferior colliculus; CN: cochlear nucleus. (For interpretation of the references to color in this figure legend, the reader is referred to the web version of this article.)

significantly higher in the HI group than in the HI + T group (Bonferroni-corrected $p = 0.05$).

4. Discussion

4.1. Sound-evoked responses in the central auditory system

Using a 3-T MRI system, activation due to sound stimulation could be detected in multiple regions in the central auditory system of hearing-impaired subjects, including the auditory cortices (AC) in the temporal lobes, the medial geniculate nuclei (MGB) in the thalamus and the inferior colliculi (IC) in the midbrain (Fig. 3). Although our sample of participants was large, no activation could be identified in the lower brainstem (CN) by means of the second-level random-effects analysis. CN activation was only detectable by means of an ROI analysis.

The ROI analysis revealed a clear level-dependency in the cortex, thalamus and midbrain (Fig. 5 and Table 3). The response in each of the auditory brain areas increased with increasing intensity of the sound stimulus, which is in agreement with earlier findings (Hall et al., 2001; Sigalovsky and Melcher, 2006; Langers et al., 2007a; Ernst et al., 2008; Lanting et al., 2008; Röhl and Uppenkamp, 2012). In normal-hearing subjects, the relation between brain activation and intensity [expressed in dB] is essentially linear in the auditory pathway (Langers et al., 2007a; Röhl and Uppenkamp, 2012). In this study, we found some indications of saturation at loud sound intensity in brainstem and thalamus responses in the hearing-impaired subjects without tinnitus (Fig. 5). Possibly, this difference is related to the reduced dynamic range ('recruitment') that is associated with sensorineural hearing loss.

Activation in the AC, MGB and IC occurred most strongly in response to stimulation of the contralateral ear (Figs. 5 and 6; Table 3). The AC is principally involved in the processing of

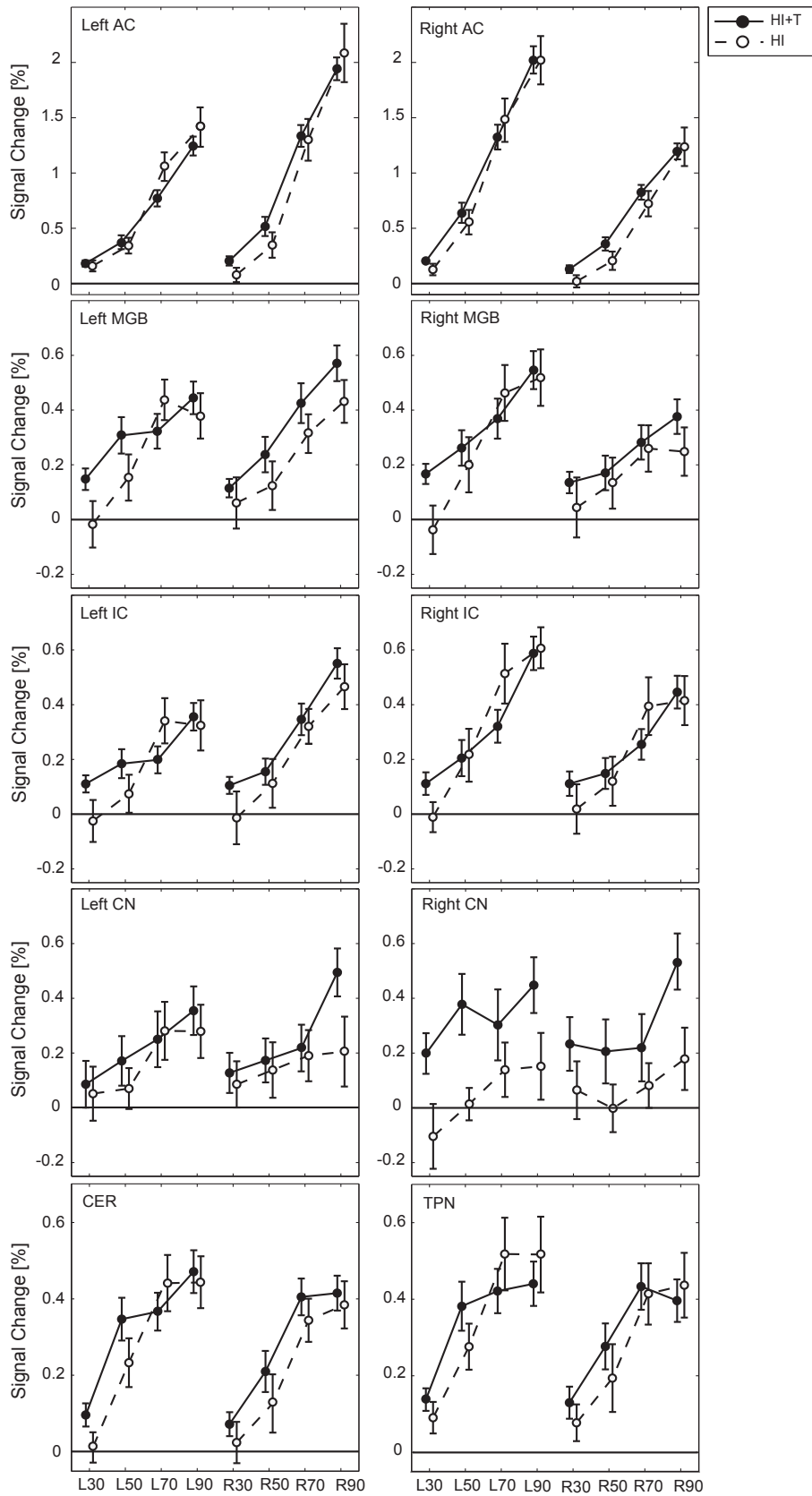


Fig. 5. The sound-evoked response amplitudes measured in ten ROIs. For each subject group separately, the response averaged across the group is plotted. Hearing-impaired subjects with tinnitus (HI + T): solid lines. Hearing-impaired subjects without tinnitus (HI): dashed lines. The error bars indicate the group standard errors around the mean. AC: auditory cortex; MGB: medial geniculate body; IC: inferior colliculus; CN: cochlear nucleus; CER: cerebellum; TPN: Task-positive network.

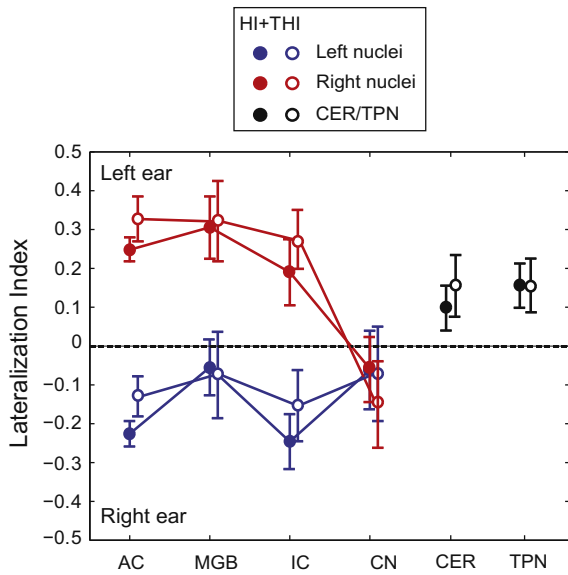


Fig. 6. The lateralization indices for the left hemispheric auditory ROIs (blue) and the right hemispheric auditory ROIs (red), the cerebellum and the task-positive network. A lateralization index > 0 indicates a response mainly to left-ear stimuli, whereas a lateralization index < 0 indicates a response mainly to right-ear stimuli. The error bars indicate the group standard errors around the mean. HI + T: hearing impairment accompanied by tinnitus; HI: hearing-impaired subjects; AC: auditory cortex; MGB: medial geniculate body; IC: inferior colliculus; CN: cochlear nucleus; CER: cerebellum; TPN: Task-positive network. (For interpretation of the references to color in this figure legend, the reader is referred to the web version of this article.)

contralateral stimuli resulting in a distinctly contralateral response preference upon monaural stimulation (Scheffler et al., 1998; Suzuki et al., 2002; Langers et al., 2005a, 2007b; Lanting et al., 2008; Amaral and Langers, 2013). Correspondingly, for the subcortical brain areas (except the CN), the average responsiveness to the contralateral ear is larger than that to stimulation of the ipsilateral ear (see also, Melcher et al., 2000; Langers et al., 2005b; Lanting et al., 2008).

The lateralization of responses was stronger in the controls, although this difference was not significant (Fig. 6). Also, the enhanced sound-evoked activations in the right CN and left MGB of tinnitus patients suggest that there are differences in the subcortical areas between tinnitus subjects and controls. Notably, the

majority of the tinnitus subjects reported nonlateralized tinnitus. Unfortunately, these differences are hard to interpret at present.

4.2. Functional connectivity patterns in the cortical, thalamic and subcortical regions

A functional connectivity analysis was performed. Functional connectivity is a statement about observed correlations between the patterns of activity in two brain areas (Friston, 1994; Smith et al., 2009). We observed that for all connections between ROIs in the model, significantly non-zero Pearson correlation coefficients were found (Fig. 7). Such a correlation does not necessarily indicate a direct connection between two correlated brain areas. It does not comment on how these correlations are mediated. In the present study, functional connectivity is likely to be substantially stimulus-induced or task-related. Since functional connectivity reflects the temporal correlation between pairs of time signals from two spatially remote areas (Friston, 1994), much of the correlation could be driven by the experimental paradigm. The experimental paradigm consisted of auditory stimuli, which may explain the high correlations between the auditory ROIs. Additionally, the subjects were instructed to press a button when an auditory stimulus was heard, which may explain the high correlations between the auditory and non-auditory ROIs.

The functional connectivity analysis showed two clusters of brain structures (Fig. 7). Those brain structures were mutually correlated within the respective cluster. The first cluster consisted of the brainstem and thalamic nuclei, which showed highly correlated activity patterns. The second cluster contained the thalamic and cortical areas. The activity in these areas showed a highly correlated response as well. Thus, the thalamus is part of both clusters, which is consistent with a function as a relay station between the brainstem and cortex (Langers and Melcher, 2011).

The observed clustering could be related to temporal differences of the response properties of the various brain areas (for a review, see Eggermont, 2001). While subcortical regions show a sustained response to sound stimuli, thus faithfully follow the sound on/off periods, the cortex mainly responds to the onset and offset of a stimulus, thus shows peaked activations at stimulus transitions (Harms and Melcher, 2003; Sigalovsky and Melcher, 2006). Correlations among centers with similar responses will be high, while responses between centers with different types of neural responses will be comparatively weak. We are unable to distinguish between

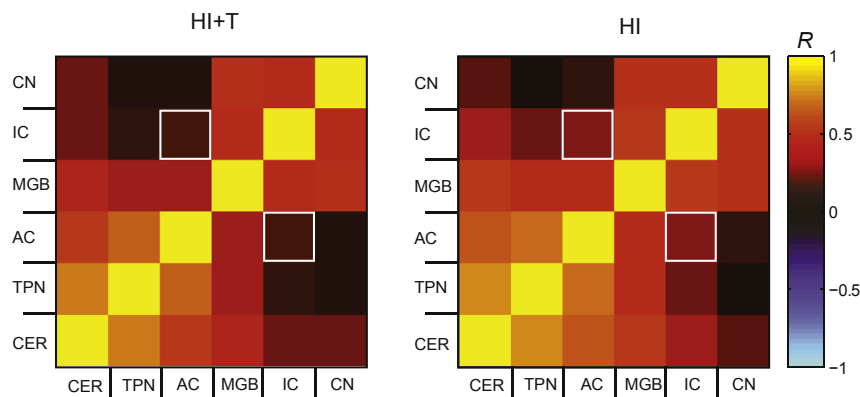


Fig. 7. Functional connectivity patterns in the HI + T and the HI group. The color-coding indicates the value of the coefficient of the Pearson correlations (R) between the respective ROIs. Correlation coefficients were significantly different between both groups for the connection between the IC and AC (indicated by a white outlined square). HI + T: hearing impairment accompanied by tinnitus; HI: hearing-impaired subjects; AC: auditory cortex; MGB: medial geniculate body; IC: inferior colliculus; CN: cochlear nucleus; CER: cerebellum; TPN: Task-positive network. (For interpretation of the references to color in this figure legend, the reader is referred to the web version of this article.)

the two types of behavior directly because the short duration of sound blocks (~8 s) in combination with the sparse sampling prevents us from differentiating onset/offset and sustained response contributions. Nevertheless, the clustering we observed seems to be consistent with the diverging response properties in different anatomic regions of the brain.

A further difference in the properties of subcortical and cortical areas, respectively, is reflected by the relation between hearing loss and response amplitudes. While the activation in subcortical areas was significantly diminished for larger hearing losses (Table 3), such a relation was not present in the auditory cortex and TPN. This suggests that the subcortical areas retained a stimulus representation that reflects the detected stimulus level above threshold, whereas the auditory cortex adapted to the reduced dynamic range caused by peripheral hearing loss. This is consistent with adaptation in monaural deafness that occurs primarily at the level of the cortex (Langers et al., 2005b).

4.3. Tinnitus-related thalamic dissociation

In tinnitus patients, the correlation coefficient between the cortical and subcortical clusters was diminished relative to the controls (Fig. 7). Since the connection between both clusters is formed by the thalamus, this difference in functional connectivity can be interpreted as a thalamic dysfunction. Interestingly, two models on tinnitus attribute a specific function to the thalamus in the pathophysiology of tinnitus.

The first model (Rauschecker et al., 2010; Zhang, 2013) assumes that the thalamic function is under the control of a subcallosal area consisting of the nucleus accumbens and ventromedial prefrontal cortex, relayed via the thalamic reticular nucleus. Abnormal gray matter volume and hyperactivity of this area (Mühlau et al., 2006; Leaver et al., 2011) have been hypothesized to lead to abnormal thalamus function causing tinnitus. Our subjects all had a sensorineural hearing loss, which may have caused abnormal neural activity in the brainstem. In subjects with hearing loss but no tinnitus, this abnormal neural input is blocked by the MGB under the control of the thalamic reticular nucleus. If thalamic gating is impaired, the abnormal brainstem activity may be passed on to the cortex resulting in tinnitus. The abnormal gating in the thalamus of tinnitus patients may also have affected the responses to sound. Specifically, the abnormal connectivity between cortical and subcortical brain areas that we observed in the tinnitus patients is possibly related to an abnormality in thalamic gating.

The second model (Llinás et al., 1999) was designed to account for abnormal dysrhythmia observed in the EEG of tinnitus patients. The model assumes that the thalamus in tinnitus patients resides in a hypo-energetic state, which was recently confirmed in patients with gaze-evoked tinnitus (van Gendt et al., 2012). The hypo-energetic state is associated with low-frequency bursting activity that is observed in the EEG as an increase of the theta rhythm. It is conceivable that this bursting mode of the thalamus also affects the response of the auditory system to an external sound stimulus. The thalamus may less accurately transmit acoustic information from the inferior colliculus to the auditory cortex. Possibly, this accounts for the abnormal connectivity between cortical and subcortical areas, as observed in the present paper.

Richardson et al. (2012) report the MGB as “a compelling structure for tinnitus research”. In their review, the role of the MGB in tinnitus is mostly explained with reference to its inhibitory afferents from the inferior colliculus and thalamic reticular nucleus. Additionally, pharmacological intervention by some selective compounds that enhance tonic inhibition, suggesting that the MGB is their main targeting site, is proposed as treatment of auditory pathologies including temporal processing disorders or tinnitus

(Richardson et al., 2012). Our results may provide a functional correlate for tinnitus treatment, which can be monitored during such interventions.

4.4. The role of non-auditory areas in our experimental paradigm

The CER and TPN were included in our analysis, since their activity correlated extensively with activation in the auditory cortex (Fig. 4). In previous research, connections between these regions were reported as well (Hunter et al., 2006; Farhadi et al., 2010; Maudoux et al., 2012). Both regions have been associated with motor control and executive functions (Ghez and Fahn, 1985; Schmahmann and Sherman, 1998; Bush et al., 2000). The TPN consists of brain regions that generally show increased activity during goal-directed behavior. Activity in the TPN is thought to be anticorrelated with activity in the default mode network (DMN) (Fox et al., 2005). The observed responses in CER and TPN may be related to the button pressing that subjects performed while listening to the experimental stimuli. Evidence in favor of this interpretation is given by activation observed in only the left parietal lobe, and by stronger activation in the right cerebellum than in the left cerebellum (Fig. 3). This activation pattern is possibly visible due to the fact that subjects responded with the right thumb whenever they perceived a sound. Furthermore, in contrast to the responses in the auditory ROIs, which increased with increasing presentation level, the responses in TPN and CER plateaued at the level of 70 dB SPL. This plateau may well be due to the fact that subjects already pressed buttons in nearly 100% of all trials for the 70 dB condition (Table 2), such that a further increase at 90 dB was impossible.

In contrast with the TPN, the cerebellum appears to play a role in nonmotor behavior (for a review see Strick et al., 2009), but also in auditory processing specifically (Petacchi et al., 2005). A cross-study meta-analysis revealed evidence for activation in five cerebellar areas during active and passive listening. Specifically to tinnitus, elevated neural activity in rats (Brozoski et al., 2007) and decreased activation during residual inhibition of the tinnitus in humans (Osaki et al., 2005) were detected in the cerebellum. Besides, in contrast to normal-hearing subjects, no significant response to sound in the cerebellum was found in tinnitus patients (Lanting et al., 2010). Our study contributes another example to these findings, although it remains difficult to interpret the role of the cerebellum in tinnitus.

4.5. Hyperacusis as a possible confound

Even though our two hearing-impaired groups were well matched in terms of hearing loss such that the principal difference between these two groups was the presence or absence of tinnitus, we cannot definitively assert that the differences in functional connectivity shown are merely due to tinnitus. Considering the significant difference in HQ scores, the between-group differences seen here could be due to hyperacusis as well. Hyperacusis as such was not an inclusion criterion, but a subject characteristic. It is very hard to untangle the effects of hyperacusis and tinnitus since these characteristics were correlated ($R = 0.61$). In order to clearly distinguish the effects of hyperacusis from those of tinnitus, a larger study including a tinnitus subgroup suffering from hyperacusis and an additional tinnitus subgroup without hyperacusis would be necessary.

5. Conclusion

We investigated brain responses to sound in subjects with a mild to moderate sensorineural hearing loss, of which a subgroup suffered from tinnitus. The tinnitus and non-tinnitus subject

groups were matched with respect to the degree of hearing loss. The most conspicuous differences between the subjects with tinnitus and those without were observed in an analysis of the functional connectivity between brain regions, rather than in the amplitudes of the sound-evoked responses. Specifically, the functional connectivity between the brainstem and cortex was lower in the tinnitus patients. This lower functional connectivity is consistent with tinnitus models proposed by Llinás et al. (1999), Rauschecker et al. (2010) and Zhang (2013).

Acknowledgments

This research was supported by the American Tinnitus Association and the Heinsius Houbolt Foundation. Dave R. M. Langers was funded by VENI research grant 016.096.011 from the Netherlands Organisation for Scientific Research and the Netherlands Organisation for Health Research and Development (ZonMw). The study is part of the research program of our department: Healthy Aging and Communication.

References

- Adjajian, P., Sereda, M., Hall, D.A., 2009. The mechanisms of tinnitus: perspectives from human functional neuroimaging. *Hear. Res.* 253, 15–31.
- Amaral, A., Langers, D.R., 2013. The relevance of task-irrelevant sounds: hemispheric lateralization and interactions with task-relevant streams. *Front. Neurosci.* <http://dx.doi.org/10.3389/fnins.2013.00264>.
- Baguley, D.M., 2003. Hyperacusis. *J. R. Soc. Med.* 96, 582–585.
- Baumgart, F., Kaulisch, T., Tempelmann, C., Gaschler-Markefski, B., Tegeler, C., Schindler, F., Stiller, D., Scheich, H., 1998. Electrodynamic headphones and woofers for application in magnetic resonance imaging scanners. *Med. Phys.* 25, 2068–2070.
- Boyen, K., Langers, D.R.M., de Kleine, E., van Dijk, P., 2013. Gray matter in the brain: differences associated with tinnitus and hearing loss. *Hear. Res.* 295, 67–78.
- Brozoski, T.J., Ciobanu, L., Bauer, C.A., 2007. Central neural activity in rats with tinnitus evaluated with manganese-enhanced magnetic resonance imaging (MEMRI). *Hear. Res.* 228, 168–179.
- Bush, G., Luu, P., Posner, M.I., 2000. Cognitive and emotional influences in anterior cingulate cortex. *Trends Cogn. Sci.* 4, 215–222 (Regul. Ed.).
- Dobie, R.A., 2003. Depression and tinnitus. *Otolaryngol. Clin. North Am.* 36, 383–388.
- Eggermont, J.J., 2001. Between sound and perception: reviewing the search for a neural code. *Hear. Res.* 157, 1–42.
- Ernst, S.M.A., Verhey, J.L., Uppenkamp, S., 2008. Spatial dissociation of changes of level and signal-to-noise ratio in auditory cortex for tones in noise. *NeuroImage* 43, 321–328.
- Farhadi, M., Mahmoudian, S., Saddadi, F., Karimian, A.R., Mirzaee, M., Ahmadizadeh, M., Ghasemikhan, K., Gholami, S., Ghoreyshi, E., Shamshiri, A., Madani, S., Bakaev, V., Moradkhani, S., Raeisali, G., 2010. Functional brain abnormalities localized in 55 chronic tinnitus patients: fusion of SPECT coincidence imaging and MRI. *J. Cereb. Blood Flow Metab.* 30, 864–870.
- Fox, M.D., Snyder, A.Z., Vincent, J.L., Corbetta, M., Van Essen, D.C., Raichle, M.E., 2005. The human brain is intrinsically organized into dynamic, anticorrelated functional networks. *Proc. Natl. Acad. Sci. U. S. A.* 102, 9673–9678.
- Friston, K.J., 1994. Functional and effective connectivity in neuroimaging: a synthesis. *Hum. Brain Mapp.* 2, 56–78.
- Ghez, C., Fahn, S., 1985. The cerebellum. In: *Principles of Neural Science*, second ed. Elsevier, New York, pp. 833–852.
- Good, P., 2002. Extensions of the concept of exchangeability and their applications. *J. Mod. Appl. Stat. Methods* 1, 243–247.
- Gu, J.W., Halpin, C.F., Nam, E.C., Levine, R.A., Melcher, J.R., 2010. Tinnitus, diminished sound-level tolerance, and elevated auditory activity in humans with clinically normal hearing sensitivity. *J. Neurophysiol.* 104, 3361–3370.
- Hall, D.A., Haggard, M.P., Akeroyd, M.A., Palmer, A.R., Summerfield, A.Q., Elliott, M.R., Guney, E.M., Bowtell, R.W., 1999. “Sparse” temporal sampling in auditory fMRI. *Hum. Brain Mapp.* 7, 213–223.
- Hall, D.A., Haggard, M.P., Summerfield, A.Q., Akeroyd, M.A., Palmer, A.R., Bowtell, R.W., 2001. Functional magnetic resonance imaging measurements of sound-level encoding in the absence of background scanner noise. *J. Acoust. Soc. Am.* 109, 1559–1570.
- Harms, M.P., Melcher, J.R., 2003. Detection and quantification of a wide range of fMRI temporal responses using a physiologically-motivated basis set. *Hum. Brain Mapp.* 20, 168–183.
- Hoffman, H.J., Reed, G.W., 2004. Epidemiology of tinnitus. In: Snow Jr., J.B. (Ed.), *Tinnitus: Theory and Management*. B.C. Decker, Inc., Hamilton, Ontario, pp. 16–41.
- Hunter, M.D., Eickhoff, S.B., Miller, T.W., Farrow, T.F., Wilkinson, I.D., Woodruff, P.W., 2006. Neural activity in speech-sensitive auditory cortex during silence. *Proc. Natl. Acad. Sci. U. S. A.* 103, 189–194.
- Khalifa, S., Dubal, S., Vuillet, E., Perez-Diaz, F., Jouvent, R., Collet, L., 2002. Psychometric normalization of a hyperacusis questionnaire. *ORL J. Otorhinolaryngol. Relat. Spec.* 64, 436–442.
- Langers, D.R.M., Backes, W.H., van Dijk, P., 2003. Spectrotemporal features of the auditory cortex: the activation in response to dynamic ripples. *NeuroImage* 20, 265–275.
- Langers, D.R.M., Van Dijk, P., Backes, W.H., 2005a. Interactions between hemodynamic responses to scanner acoustic noise and auditory stimuli in functional magnetic resonance imaging. *Magn. Reson. Med.* 53, 49–60.
- Langers, D.R.M., van Dijk, P., Backes, W.H., 2005b. Lateralization, connectivity and plasticity in the human central auditory system. *NeuroImage* 28, 490–499.
- Langers, Dave R.M., van Dijk, P., Schoenmaker, E.S., Backes, W.H., 2007a. fMRI activation in relation to sound intensity and loudness. *NeuroImage* 35, 709–718.
- Langers, D.R.M., Backes, W.H., van Dijk, P., 2007b. Representation of lateralization and tonotopy in primary versus secondary human auditory cortex. *NeuroImage* 34, 264–273.
- Langers, D.R.M., Melcher, J.R., 2011. Hearing without listening: functional connectivity reveals the engagement of multiple nonauditory networks during basic sound processing. *Brain Connectivity* 1, 233–244.
- Langers, D.R.M., van Dijk, P., 2011. Mapping the tonotopic organization in human auditory cortex with minimally salient acoustic stimulation. *Cereb. Cortex* 55.
- Lanting, C.P., De Kleine, E., Bartels, H., Van Dijk, P., 2008. Functional imaging of unilateral tinnitus using fMRI. *Acta Otolaryngol.* 128, 415–421.
- Lanting, C.P., de Kleine, E., Eppinga, R.N., van Dijk, P., 2010. Neural correlates of human somatosensory integration in tinnitus. *Hear. Res.* 267, 78–88.
- Lanting, C.P., de Kleine, E., van Dijk, P., 2009. Neural activity underlying tinnitus generation: results from PET and fMRI. *Hear. Res.* 255, 1–13.
- Leaver, A.M., Renier, L., Chevillet, M.A., Morgan, S., Kim, H.J., Rauschecker, J.P., 2011. Dysregulation of limbic and auditory networks in tinnitus. *Neuron* 69, 33–43.
- Liu, R.Y., 1988. Bootstrap procedures under some non-I.I.D. models. *Ann. Statist.* 16, 1696–1708.
- Llinás, R.R., Ribary, U., Jeanmonod, D., Kronberg, E., Mitra, P.P., 1999. Thalamocortical dysrhythmia: a neurological and neuropsychiatric syndrome characterized by magnetoencephalography. *Proc. Natl. Acad. Sci. U. S. A.* 96, 15222–15227.
- Lockwood, A.H., Salvi, R.J., Burkard, R.F., 2002. Tinnitus. *N. Engl. J. Med.* 347, 904–910.
- Maldjian, J.A., Laurienti, P.J., Kraft, R.A., Burdette, J.H., 2003. An automated method for neuroanatomic and cytoarchitectonic atlas-based interrogation of fMRI data sets. *NeuroImage* 19, 1233–1239.
- Maudoux, A., Lefebvre, P., Cabay, J.E., Demertzi, A., Vanhauudenhuysse, A., Laureys, S., Soddu, A., 2012. Auditory resting-state network connectivity in tinnitus: a functional MRI study. *PLoS ONE* 7, e36222.
- Melcher, J.R., Levine, R.A., Bergevin, C., Norris, B., 2009. The auditory midbrain of people with tinnitus: abnormal sound-evoked activity revisited. *Hear. Res.* 257, 63–74.
- Melcher, J.R., Sigalovsky, I.S., Guinan, J.J., Levine, R.A., 2000. Lateralized tinnitus studied with functional magnetic resonance imaging: abnormal inferior colliculus activation. *J. Neurophysiol.* 83, 1058–1072.
- Mühlau, M., Rauschecker, J.P., Oestreicher, E., Gaser, C., Röttinger, M., Wohlschläger, A.M., Simon, F., Etgen, T., Conrad, B., Sander, D., 2006. Structural brain changes in tinnitus. *Cereb. Cortex* 16, 1283–1288.
- Newman, C.W., Jacobson, G.P., Spitzer, J.B., 1996. Development of the tinnitus handicap inventory. *Arch. Otolaryngol. Head Neck Surg.* 122, 143–148.
- Nichols, T.E., Holmes, A.P., 2002. Nonparametric permutation tests for functional neuroimaging: a primer with examples. *Hum. Brain Mapp.* 15, 1–25.
- Noreña, A.J., Eggermont, J.J., 2003. Changes in spontaneous neural activity immediately after an acoustic trauma: implications for neural correlates of tinnitus. *Hear. Res.* 183, 137–153.
- Norman-Haignere, S., Kanwisher, N., McDermott, J., 2013. Cortical pitch regions in humans respond primarily to resolved harmonics and are located in specific tonotopic regions of anterior auditory cortex. *J. Neurosci.* 33, 19451–19469.
- Oldfield, R.C., 1971. The assessment and analysis of handedness: the Edinburgh inventory. *Neuropsychologia* 9, 97–113.
- Osaki, Y., Nishimura, H., Takasawa, M., Imaizumi, M., Kawashima, T., Iwaki, T., Oku, N., Hashikawa, K., Doi, K., Nishimura, T., Hatazawa, J., Kubo, T., 2005. Neural mechanism of residual inhibition of tinnitus in cochlear implant users. *Neuroreport* 16, 1625–1628.
- Petacchi, A., Laird, A.R., Fox, P.T., Bower, J.M., 2005. Cerebellum and auditory function: an ALE meta-analysis of functional neuroimaging studies. *Hum. Brain Mapp.* 25, 118–128.
- Rauschecker, J.P., Leaver, A.M., Mühlau, M., 2010. Tuning out the noise: limbic-auditory interactions in tinnitus. *Neuron* 66, 819–826.
- Richardson, B.D., Brozoski, T.J., Ling, L.L., Caspary, D.M., 2012. Targeting inhibitory neurotransmission in tinnitus. *Brain Res.* 1485, 77–87.
- Röhl, M., Uppenkamp, S., 2012. Neural coding of sound intensity and loudness in the human auditory system. *J. Assoc. Res. Otolaryngol.* 13, 369–379.
- Rosenbaum, P.R., 2005. An exact distribution-free test comparing two multivariate distributions based on adjacency. *J. R. Statist. Soc. B* 67, 515–530.
- Scheffler, K., Bilecen, D., Schmid, N., Tschopp, K., Seelig, J., 1998. Auditory cortical responses in hearing subjects and unilateral deaf patients as detected by functional magnetic resonance imaging. *Cereb. Cortex* 8, 156–163.
- Schmahmann, J.D., Sherman, J.C., 1998. The cerebellar cognitive affective syndrome. *Brain* 121 (Pt 4), 561–579.

- Seki, S., Eggermont, J.J., 2003. Changes in spontaneous firing rate and neural synchrony in cat primary auditory cortex after localized tone-induced hearing loss. *Hear. Res.* 180, 28–38.
- Sigalovsky, I.S., Melcher, J.R., 2006. Effects of sound level on fMRI activation in human brainstem, thalamic and cortical centers. *Hear. Res.* 215, 67–76.
- Smith, S.M., Fox, P.T., Miller, K.L., Glahn, D.C., Fox, P.M., Mackay, C.E., Filippini, N., Watkins, K.E., Toro, R., Laird, A.R., Beckmann, C.F., 2009. Correspondence of the brain's functional architecture during activation and rest. *Proc. Natl. Acad. Sci. U. S. A.* 106, 13040–13045.
- Strick, P.L., Dum, R.P., Shetake, J.A., 2009. Cerebellum and nonmotor function. *Annu. Rev. Neurosci.* 32, 413–434.
- Suzuki, M., Kitano, H., Kitanishi, T., Itou, R., Shiino, A., Nishida, Y., Yazawa, Y., Ogawa, F., Kitajima, K., 2002. Cortical and subcortical activation with monosyllabic stimulation by functional MRI. *Hear. Res.* 163, 37–45.
- van Gendt, M.J., Boyen, K., de Kleine, E., Langers, D.R., van Dijk, P., 2012. The relation between perception and brain activity in gaze-evoked tinnitus. *J. Neurosci.* 32, 17528–17539.
- Wu, C.F.J., 1986. Jackknife, bootstrap and other resampling methods in regression analysis. *Ann. Statist.* 14, 1261–1295.
- Zhang, J., 2013. Auditory cortex stimulation to suppress tinnitus: mechanisms and strategies. *Hear. Res.* 295, 38–57.